

In-situ Thermal Performance Monitoring of Pharma 4.0 Flow Bioreactors

Kristóf Hegedűs¹, Gusztáv Hantos^{1,2}, Tamás Pardy³, Ferenc Ender^{1,2}

¹ Department of Electron Devices, Budapest University of Technology and Economics

² Spinsplit LLC, Budapest, Hungary

³ Thomas Johann Seebeck Department of Electronics, Tallinn University of Technology

hegedus.kristof | ender.ferenc @ vik.bme.hu, hantos @ spinsplit.com, tamas.pardy @ taltech.ee

Abstract

Pharma 4.0 is an application of Industry 4.0 principles to pharmaceutical industry. Flow chemistry is a method to carry out chemical reactions under well-controlled conditions in small volume reactors. Reactions carried out in the flow chemistry system are supervised under continuous quality control may satisfy some of the prerequisites of Pharma 4.0 systems. In the present work the thermal interface quality of a chemical reactor assembled to a flow chemistry thermostat was investigated to detect user related assembly errors and thermal interface degradation over time. We were able to mimic a designed contamination of the thermal interface material caused by inadequate assembly as a result of glass spacers inserted between the reactor and the heat exchanger plate. The thermal resistance was characterized in several measurement setups to determine the smallest detectable change of the thermal interface. Measurements have shown that even 0.05 K/W change in thermal resistance is detectable by the investigated thermostat unit.

1 Background

Flow chemistry is a method to carry out chemical reactions under well-controlled conditions in small volume reactors. Flow chemistry instruments provide determined environmental conditions (e.g. pressure, temperature, flow rate) in small, well-controlled volumes called flow bioreactors. A flow thermostat, an example of such devices, is the focus of our present work. Flow thermostats are designed to provide homogeneous temperature distribution in small volume flow reactors, as required by the aimed chemical reactions. To provide the necessary level of versatility, flow reactors are not permanently assembled on the heat exchanger, but they are interchangeable. Therefore the operators have the freedom to choose and assemble the most suitable flow reactor (e.g. microchip reactor, tubular reactor, disc reactor, column reactor etc.). Reliable thermal interfacing between the assembled reactor and the heat exchanger is of highest importance, yet human errors cannot be neglected during the assembly process.

As a prerequisite of Pharma 4.0, the reactions carried out in the flow chemistry system are supervised under continuous quality control [1, 2]. To achieve this, number of sensors and methods are deployed in the system to measure physical quantities. Our ambition is to demonstrate a method to monitor the quality of a thermal interface between the thermostat and the bioreactor, and therefore, to predict the need of maintenance [5].

2 Methodology

2.1 Thermal system

The thermostat is a *thermo-electric heat pump (TEH)*, with one side facing inside the chassis and equipped with a forced convection heat sink, called *passive side*. The *working side* of the TEH is facing outwards, providing a thermal interface for

the bioreactor assembly. Therefore, the operator can change the reactor according to the actual reaction type (e.g. a bioreactor chip holder, see *Figure 1*).

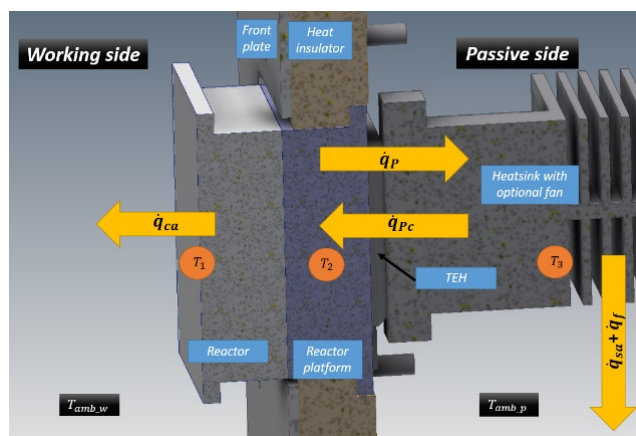


Figure 1: Cross-section view of the system under study with domains, interfaces and boundary heat fluxes, as well as temperature sensors (T_1, T_2, T_3) shown.

The physical and simulated structural elements of the assembled thermostat unit contain the following main parts:

- *TEH*: 2 Peltier cells located next to each other, simulated as a heat pump element
- *Reactor platform*: located between the *TEH* and the *Reactor*
- *Reactor*: an interchangeable part of the system which is assembled on the *reactor platform*
- *Heat insulator*: insulates the heat transfer towards the front plate
- *Front plate*: mounting plate for the structural elements listed above.

2.2 Thermal modelling

The thermal model detailed in this work is usable for both steady-state and transient thermal analyses, given an experimentally characterized thermostat system with well-defined structural materials and boundary conditions. The core of the model is the heater, which generates a volumetric heat flux Q , propagated through the geometry. Heat flux can be expressed with the heat transfer equation:

$$\rho C_p \nabla T - \nabla(k \nabla T) = Q \quad (1)$$

Where structural materials are characterized by their density ρ , specific heat capacity C_p , absolute temperature T and thermal conductivity k , as detailed in our concrete case Table 1. The experimental device was tested in a laboratory room, which provided a constant ambient temperature ($25 \pm 1^\circ\text{C}$). Therefore, ambient temperature in the model was also considered constant 25°C , as well as act as the initial temperature value in the model.

Four dominant heat transfer paths were identified in the structure, where each heat flux was a vector with direction as marked in Figure 1 (normal to the surface through which it passes): q_{sa} (heat rejection by the heat sink), q_p (heat forced through the Peltier cell), q_{pc} (heat backflow from heat spreader to reactor side), q_{ca} (conv. heat loss to ambient on reactor side). Ambient temperatures (T_{amb_w} , T_{amb_p}) were fixed at 25°C in the model. The static temperature simulation was done with different heating powers and TIMs (thermal interface materials).

The boundary conditions of the thermal model were as follows:

- Boundary heat source (normal direction heat flux of the Peltier cells): input heat of the system (Power [W]), the passive side is not part of the thermal model
- Heat flux: convective heat loss on sides looking to the ambient (air)
- Thermal insulation: no heat exchange with part made of insulating material
- Temperature: front side of chip holder set to 25°C .

The mesh had 35 517 elements, the average element quality was 0.57 with size of 16 mm³. Table 1 contains the physical data of each material for the simulation.

Table 1. Materials and properties of the used parts in the thermal simulation

Name	Material	C_p [J/kg*K]	k [W/mK]	ρ [kg/m ³]
Reactor platform & Reactor	Al 6061	900	238	2700
Heat insulator	PTFE	1050	0.24	2200

The thermal simulation model was built in COMSOL Multiphysics 5.4 and Heat Transfer in Solids interface was used. The model was solved via the built-in stationary, and time-dependent solvers of COMSOL. Three-dimensional model geometry (Figure 1) was imported from Autodesk Inventor.

2.3 Experimental setup

The actual measurements were carried out with a flow chemistry thermostat module (spFlow Chem thermostat module, Spinsplit LLC, Budapest, Hungary). Geometrical CAD models of the module were provided by Spinsplit LLC.

The reactor, reactor platform and the TEH were assembled using screws, and the thermal interface was connected with a thin TIM layer. The distance between the reactor and the reactor platform part can be precisely set by placing various and homogeneous glass spheres into the TIM. Such glass spheres were ranging from 75, 250 to 500 μm , respectively. The setup without glass spacers and three cases with spacers represent four different experimental setups. These setups mimicked operator related errors during the reactor assembly. In the ideal case, a thin and homogeneous TIM layer was homogeneously distributed between the reactor and the reactor platform, providing the best possible heat transfer of the four cases. In other cases, the glass spacers mimic a given grade of TIM contamination what is likely to happen in the chemical laboratory due to human errors. With such experimental setup it was possible to identify the detection limit of the thermal interface degradation considering the measurement characteristics of the actual physical device.

2.4 Measurement method

Each measurement started with a power step function applied to the Peltier-cells, while constant input power was maintained until the thermal system reached its steady state. The time functions of the temperature sensors (T_1 , T_2 , T_3) as well as the input voltage and current were recorded. Knowing the input power (P) and the temperature difference ($\Delta T = T_1 - T_2$) between the two sides of the thermal interface, the thermal resistance (R_{th}) of the interface can be calculated as follows:

$$R_{th} = \Delta T / P \quad (2)$$

The input power (P) and the temperature difference (ΔT) were calculated by taking 30 seconds averaged samples starting from t_{ss} . Here, t_{ss} was considered as 4 times longer than the system's thermal time constant τ , i.e. steady state time $t_{ss} = 4\tau$.

The temperature difference ΔT reaches a steady value significantly earlier than the whole thermal system reaches its steady state. Therefore, we defined an optimal measurement window (OMW) as the earliest possible time when R_{th} can be calculated. OMW is a five minutes long time window within ΔT does not change in a $\pm 5\%$ range (Figure 4). R_{th} calculations were done based on the samples taken and averaged within OMW.

Temperature measurements, power settings, measurement logs were done by the software provided by Spinsplit LLC. For temperature recording, 10 k Ω NTC thermistors were used.

3 Results

3.1 Investigation of the static thermal behaviour

The experimental measurement was done on one thermal interface with 5 different TIM thicknesses. The TIM thickness was fine-tuned using solid glass microspheres as spacers. Figure 2 shows calculated and simulated ΔT values at six heating power values. The simulation was applied to the perfectly assembled thermal interface (with no spacers). The same experimental case was compared to the simulation and good matching was observed (Figure 2). Table 2 contains the statistical parameters (standard deviation and linear correlation coefficient) of the linear interpolations of each measurement and the corresponding R_{th} values were calculated.

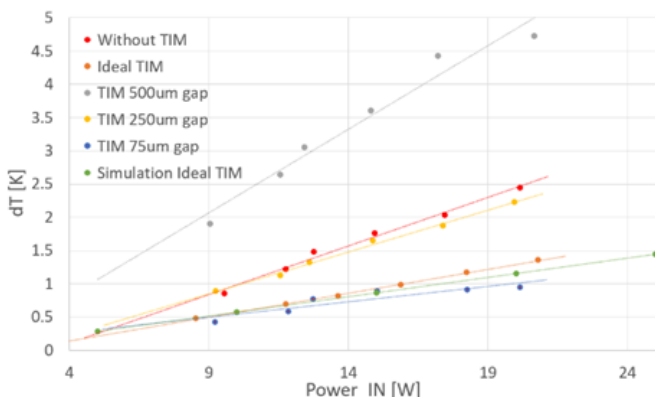


Figure 2: The temperature difference between two sides of the thermal interface, depending on the input electrical power of the Peltier-cells.

Table 2: The statistical characteristics of the linear regression of the measured and simulated points (Figure 2) and the thermal resistance deduced from them.

Name	R^2 [-]	s^2 [-]	R_{th} [K/W]
Without TIM	0.989	0.542	0.146
Ideal TIM	0.999	0.304	0.071
TIM 500 μ m gap	0.963	1.015	0.251
TIM 250 μ m gap	0.995	0.473	0.126
TIM 75 μ m gap	0.835	0.192	0.048
Simulation Ideal TIM	1.000	0.000	0.058

Figure 3 shows the calculated R_{th} values at six different heating power values. Notably, the ideal TIM case resulted the lowest, yet similar R_{th} values as the one with 75 μ m glass sphere spacers, suggesting that the initial TIM layer thickness was about 75 μ m. In case of the assembly without TIM, the

thermal resistance was higher, almost double of the one calculated for the ideal case. As expected, by increasing the spacer sphere size and therefore the TIM was more degraded, the thermal resistance was increased.

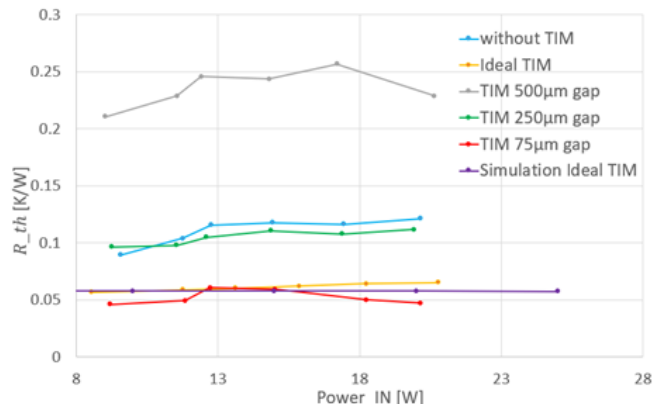


Figure 3: Experimental and simulated results of the thermal resistance of the thermal interface, depending on the input electrical power of the Peltier-cells.

3.2 Investigation of the dynamic thermal behaviour

Figure 4 shows T_1 and T_2 temperature values over time as well as their difference (ΔT) measured over time for the selected case with 500 μ m glass sphere spacers. After the power step applied, the temperature difference ΔT reached an overshoot. It is clearly visible that the OMW came significantly earlier (16 minutes) than the steady state of the system (81 minutes).

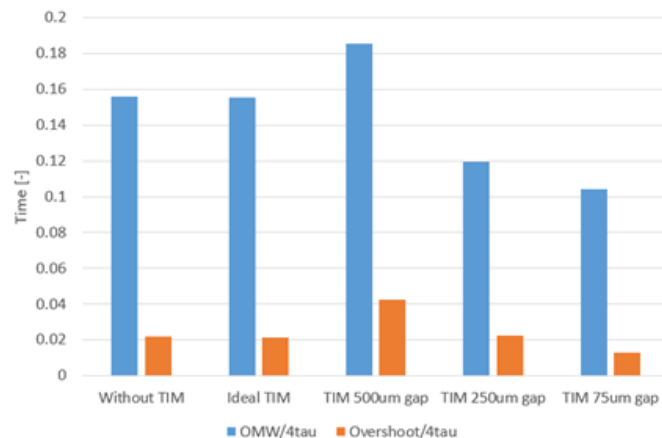


Figure 4: ΔT versus time (top), temperature of the two side of the thermal interface versus time (bottom), at 500 μ m glass sphere spacers

In Figure 5 the ratio of steady state time (t_{ss}) and OMW are shown for different setups.

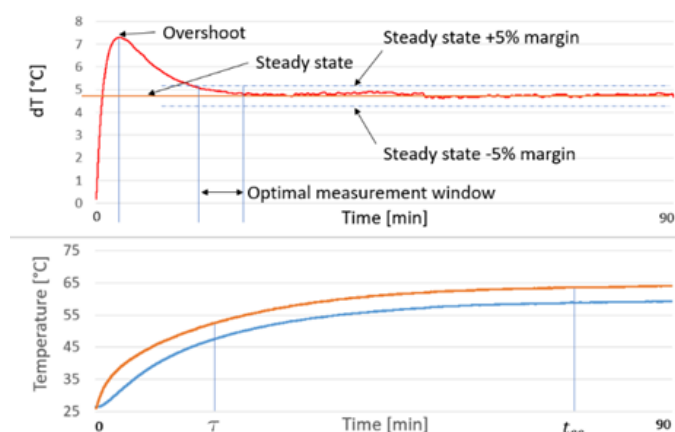


Figure 5: Optional times for decision making at different thermal interface compared to steady state time (t_{ss}) of the system

4 Discussion

The measurements showed that the degradation of the thermal interface can be mimicked by inserting glass spacers in the TIM material, and the investigated flow chemistry reactor system was able to detect 0.05 [K/W] change in the thermal resistance.

It was also concluded that the actual thermal resistance values can be determined significantly earlier (around 5 times reduction in measurement time) than the thermal system would reach its steady state. For this, we defined an optimal measurement window. We found that using OMW, the required measurement times were decreased by a factor of 5 to 10 in the investigated cases. Presumably, significant reduction in measurement time can be achieved for other reactor geometries (i.e. different thermal capacitance ratios), which should be further investigated by simulation. For a selected case, actual measurements showed a good agreement with the simulation model.

The calibrated thermal model will be used for the design of the flow chemistry thermostat with in-situ self-assessment. Continuous monitoring of the thermal interface may indicate the possible degradation of it, even due to heavy thermo cycling or poor assembly quality by the operator. This feature enables that the bioreactor assembly can monitor itself and recognize the type and value of the fault, helps to preserve the quality and reliability of chemical measurements to satisfy the requirements of Pharma 4.0.

Acknowledgements

The research reported in this paper and carried out at the Budapest University of Technology and Economics was supported by the “TKP2020, National Challenges Program” of the National Research Development and Innovation Office (BME NC TKP2020).

Literature

1. Ding, B., 2018. Pharma industry 4.0: Literature review and research opportunities in sustainable pharmaceutical supply chains. *Process Safety and Environmental Protection*, 119, pp.115-130.
2. Herwig, C., Wölbeling, C. and Zimmer, T., 2017. A holistic approach to production control. *Pharm. Eng*, 37, pp.44-46.
3. Souza, J.M., Galaverna, R., Souza, A.A.D., Brocksom, T.J., Pastre, J.C., Souza, R.O.D. and OLIVEIRA, K.T., 2018. Impact of continuous flow chemistry in the synthesis of natural products and active pharmaceutical ingredients. *Anais da Academia Brasileira de Ciências*, 90(1), pp.1131-1174.
4. Roberge, D.M., Ducry, L., Bieler, N., Cretton, P. and Zimmermann, B., 2005. Microreactor technology: a revolution for the fine chemical and pharmaceutical industries. *Chemical Engineering & Technology: Industrial Chemistry-Plant Equipment-Process Engineering-Biotechnology*, 28(3), pp.318-323.
5. V. Szekely, S. Torok, E. Nikodemusz, G. Farkas and M. Rencz, "Measurement and evaluation of thermal transients," IMTC 2001. Proceedings of the 18th IEEE Instrumentation and Measurement Technology Conference. Rediscovering Measurement in the Age of Informatics (Cat. No.01CH 37188), Budapest, 2001, pp. 210-215 vol.1, doi: 10.1109/IMTC.2001.928814.